

# **Topographic map generation from the Shuttle Radar Topography Mission C-band SCANSAR interferometry**

Scott Hensley\*, Paul Rosen and Eric Gurrola

Jet Propulsion Laboratory, 4800 Oak Grove Drive Pasadena, California 91109. MS 300-235

## **ABSTRACT**

A highly accurate global topographic map of the Earth's surface has been an elusive goal for at least three decades that may soon be achieved with the newly acquired Shuttle Radar Topographic Mission (SRTM) data. SRTM collected data for 99.97% of the Earth's landmass between  $-57^{\circ}$  and  $60^{\circ}$  latitude during an 11 day mission in February 2000. A modified version of the SIR-C radar that previously flew on the shuttle in 1994 augmented with a radar mounted on a 62 m boom was used to collect radar interferometric data at C (5.6 cm wavelength) and X (3 cm wavelength) bands. The C-band radar was operated in the SCANSAR mode in order to extend the swath width to 225 km, the minimal amount required to achieve contiguous coverage at the equator. This paper presents an overview of the new algorithms and techniques used to process the SCANSAR data to digital elevation maps. First results of topographic maps generated from the SRTM data are used to illustrate the techniques described in this paper.

**Keywords:** SRTM, SCANSAR, interferometry, topography, mapping, DEM

## **1. INTRODUCTION**

In February 2000 the Shuttle Radar Topography Mission (SRTM) carried out a mission to map the world's landmass between  $\pm 60^{\circ}$  using radar interferometry<sup>1</sup>. The radar-mapping instrument consisted of modified versions of the SIR-C C-band and X-band radars flown on the shuttle in 1994. Modifications to the SIR-C radars included a 60 m retractable boom equipped with C-band and X-band receive only antennas attached to the boom's end. Additional metrology systems designed to measure the shuttle position and attitude as well as the position of the boom antennas to high accuracy was also added. To map the world in the 10 days allotted for the mission required the C-band radar to operate in ScanSAR mode. The C-band interferometry data was collected in swaths comprised of four subswaths each as shown in Figure 1. ScanSAR mapping modes alternately switch between two (or more) beam positions in the cross track direction to increase the swath width at the expense of along track resolution. Exploiting the C-band polarization capability, the SRTM C-band radar operated in ScanSAR mode on vertical (V) and horizontal (H) polarizations to achieve an effective swath width of 225 km while maximizing the SNR over the swath.

Operational processing of the C-band ScanSAR interferometric data into a seamless topographic map required several processor innovations. In this paper we present an overview of the SRTM processor and show examples of SRTM processed data.

## **2. SYSTEM OVERVIEW**

Constructing accurate height maps using radar interferometry requires precise knowledge of the platform position, attitude, and interferometric baseline as well as knowledge of the radar operating parameters<sup>2</sup>. Table I provides a list of the

major system parameters. To meet these stringent requirements, the SRTM mapping instrument was equipped with a specially designed motion measurement system. Absolute position information was determined from two GPS receivers

**Table I** SRTM System Parameters

Parameter	Value
Baseline Length	62 m
Baseline Orientation Angle	45°
Wavelength	.0566 m
Burst Length	60 –100 pulses
Platform Altitude	240 km
Platform Velocity	7.5 km/s
Look Angle Range	30°-60°
Antenna Lengths	12 m/8 m
PRF Range	1330 - 1550 Hz

located on the outboard antenna. Attitude information was derived from a combination of star tracker and IRU measurements. The interferometric baseline (vector between the inboard and outboard antennas) was measured using a combination of an optical target tracker, which measured the angles to several targets located on the outboard antenna structure; and an electronic ranging device used to measure the distance between inboard and outboard antennas. The motion measurement system is part of the Attitude and Orbit Determination Avionics (AODA) system that reduced all the motion measurements and provided that information in the AODA PADR file. The PADR file includes the correspondence between the radar clock (MET) and GPS time. This file provides the SRTM Processor with the precise timing information required to align the pulse data with the associated motion and baseline data.

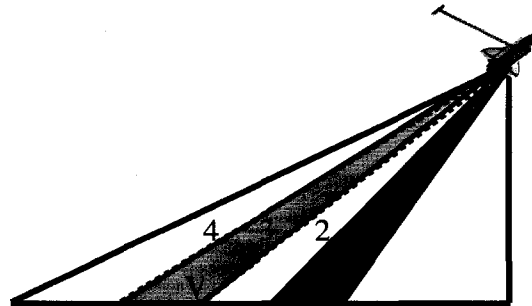


**Figure 1.** The SRTM C-band radar collects data in two subswaths simultaneously using horizontal (H) and vertical polarization (V). The four ScanSAR subswaths are numbered 1-4 starting from nadir as shown above.

### 3. PROCESSOR DESCRIPTION

Processing of the SRTM data into topographic maps can be roughly divided into three major steps as shown in Figure 2. Data collected onboard shuttle was stored on approximately 300 high density tapes that were duplicated and transcribed to a more convenient tape media prior to shipment to the Jet Propulsion Laboratory (JPL) where the data processing is to occur. In addition to the radar raw signal history data, motion measurement data collected by the AODA system, that consisted of three GPS receivers, a star tracker and IMU, an electronic distance measuring unit, and optical tracking device were downloaded and processed at JPL. These data, illustrated in the green box, are integral to accurate processing of the raw signal history data into digital elevation data by the Topographic Mapping Subsystem (TPS) shown in the red box in Figure 2. The TPS processes each subswath of each of the nearly 1000 datatakes into strip map digital elevation models (DEMs) in a special coordinate system aligned with the radar geometry called the SCH coordinate system. A datatake is comprised of the four subswaths of SCNASAR data collected from radar collection initiation, from just prior to ocean to land crossing, to radar collection termination, just after crossing from land to ocean. Strip map products generated for a subswath consist of an orthorectified C-band radar image, the elevation data in SCH coordinates, an interferometric

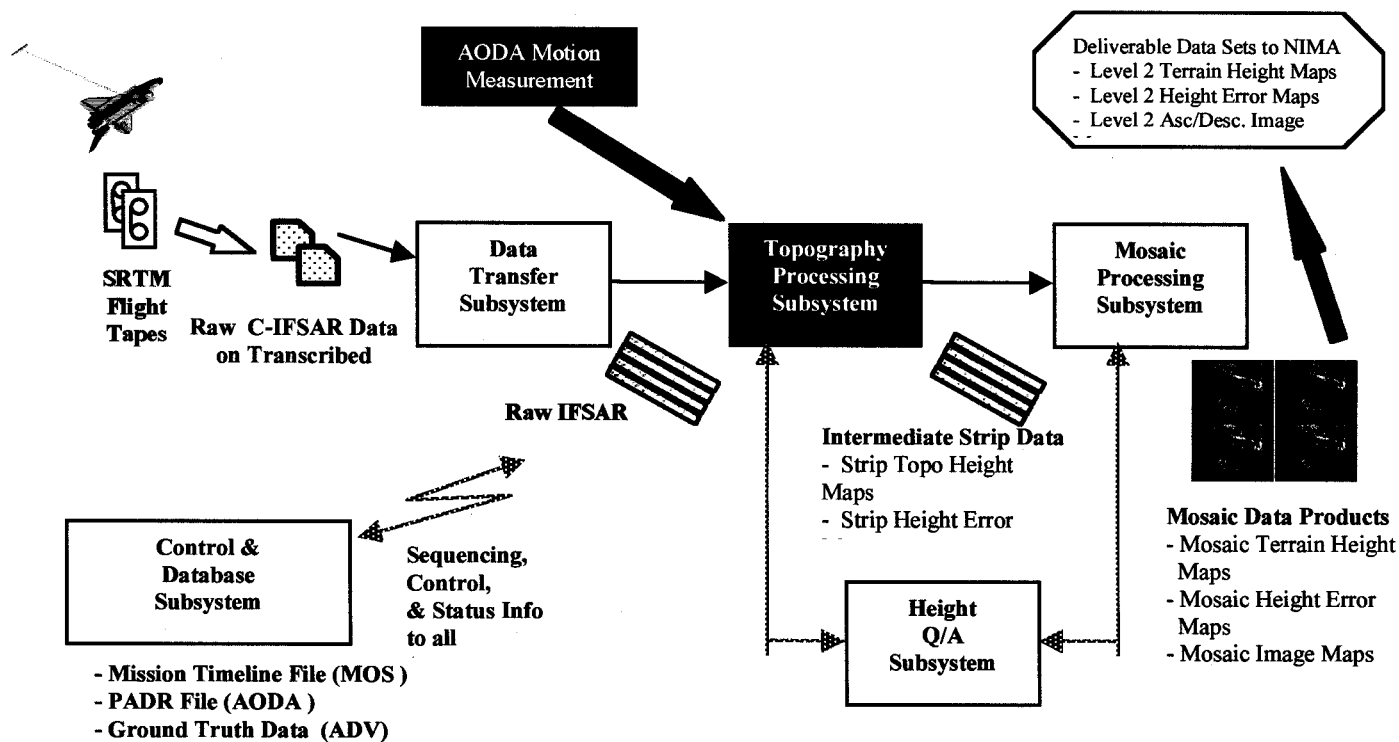


**Figure 2.** A block diagram of the SRTM data flow from raw data to completed map products. The Topographic Processing Subsystem converts the raw radar signal history data into strip maps products. Final map products are generated in the Mosaic Processing Subsystem that combines the SCH strip map data and converts it into geographic coordinates.

correlation map, and a height error map that provides an estimate of the statistical height accuracy for each point in the DEM. Interferometric correlation is a measure the similarity of radar data collected from the two radar antennas comprising the SRTM radar interferometer. Correlation can be related to the phase noise, the primary measurement used to generate height measurements, and therefore to height accuracy. It is this relationship that is exploited to generate the height error maps. Subsequent to strip map processing the data is passed to the Mosaic Processing Subsystem (MPS) where the SCH products are combined and converted into geographic coordinates. Quality assurance measures are made both after TPS and MPS processing and if anomalies are detected the data is queued for further analysis and potential reprocessing. The remainder of this paper will focus on the TPS processing.

The Topographic Processing Subsystem (TPS) is comprised of two major programs, the Preprocessor and the Processor. The Preprocessor's main function is to use inputs from AODA, the Verification and Calibration Subsystem and C-band radar command parameters to generate a Processor command file and time varying parameter file, that includes motion measurement information, in an appropriate coordinate system and format for the Processor. In the Preprocessor datatakes are subdivided into latitude bands called peg regions. Peg region boundaries were selected so that output files from each region would not exceed 2 GB in size (approximately 1500 km of along track data collection) and to minimize the amount of swath drift within the SCH coordinate system that is specified by the Preprocessor for each peg region of a datatake.

The Processor's main function is to generate strip maps from the raw radar signal history using a modified version of an algorithm<sup>3</sup> previously developed for airborne interferometric mapping applications. Modifications to the processor were designed to accommodate burst mode collection employed by the C-band radar. As explained previously the C-band radar operated in SCANSAR mode where the radar beam alternately switched mapping from two subswaths. Each group of transmit and receive pulses, nominally consisting of 50-80 pulses, is called a burst. This is to be contrasted with traditional strip mode synthetic aperture radar (SAR) systems that continuously transmit and receive pulses. In strip mode every target is illuminated for the entire azimuth (along track) beamwidth of the antenna and targets at a given range have approximately the same range (and consequently phase) history. Range and phase histories for burst mode targets depend on that portion(s) of the azimuth beamwidth that illuminated them. The spatially varying nature of the target phase history and the need to



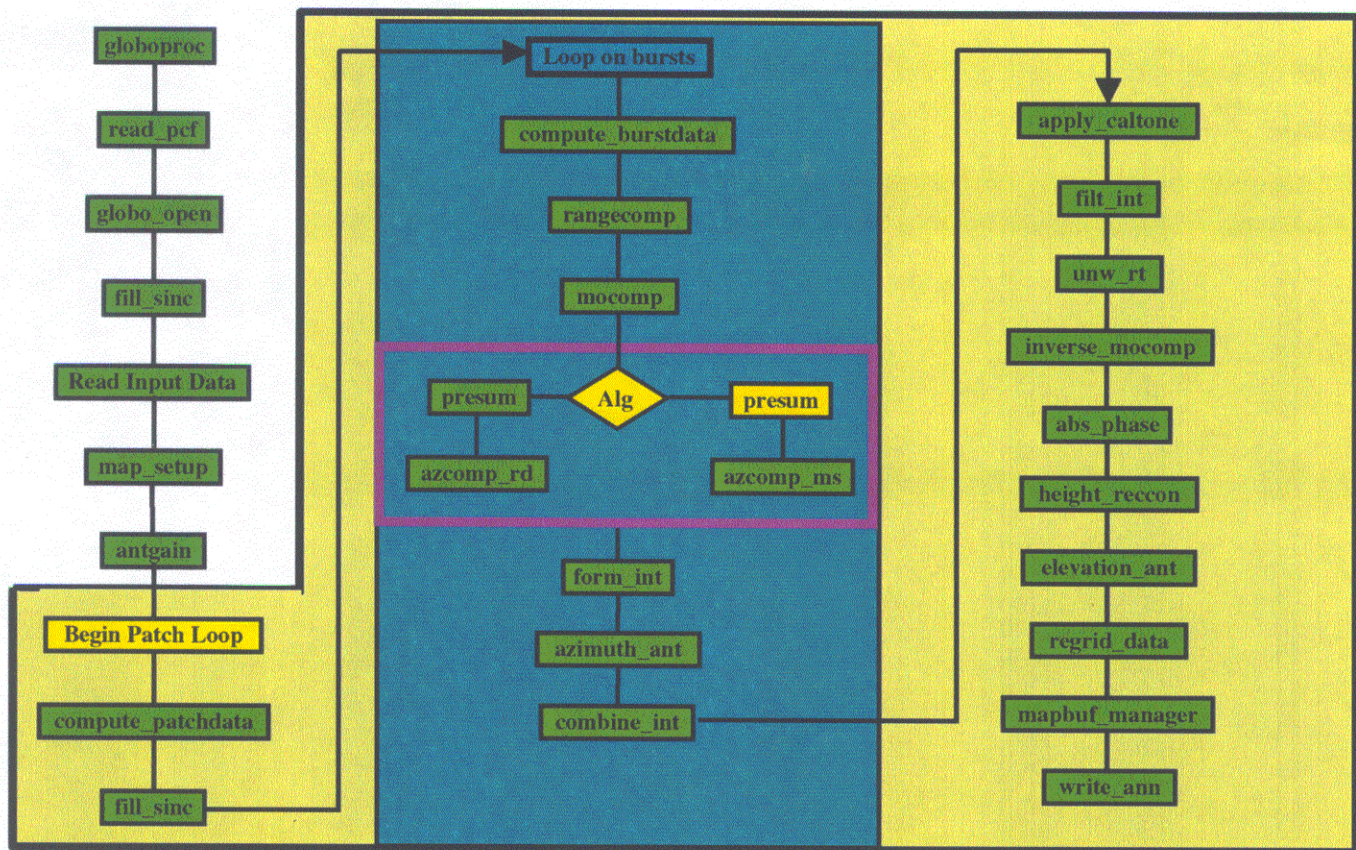


Figure 3. Block diagram of the SRTM C-Band Topographic Mapping Processor.

coherently combine the bursts into a seamless topographic map necessitate that data collected in burst mode must be processed slightly differently than the standard strip mode SAR data.

A block diagram for the SRTM C-band topographic processor (called globoproc) is given in Figure 3. The processor is patched based, that is the data to be processed is subdivided into overlapping regions called patches. Patches consist of data from approximately 50-90 bursts (around 60 km along track distance). This size of patch was primarily driven by two factors. First, the need to maintain certain data products in memory limits the size of a patch while the desire to have as long an along track region as possible to aid in unwrapping (described later) drives one to larger patches. The large green irregularly shaped region in Figure 3 shows the data processing for each patch and the turquoise block shows the processing done for each burst. A brief description of each of the major processing steps is given followed by more detailed information in the subsequent subsections.

The first processing step is decoding the byte data, followed by range compression for each of the two interferometric channels. Using the shuttle motion information obtained by the AODA subsystem, the data are compensated for perturbations in spacecraft motion from a reference path in the motion compensation module. After motion compensation the data are resampled to a uniform along track grid with presumming operation and then azimuth compressed. Two azimuth compression algorithms were implemented, a standard range-doppler algorithm (azcomp\_rd) and a modified SPECAN algorithm (azcomp\_ms). If modified SPECAN is used the presumming step can be omitted since as this can be done as part of azimuth compression with this algorithm. This generates two single-look complex images. One of the single-look complex image pair is used as reference to form a burst interferogram, (form\_int), that is obtained by multiplying the complex pixel value in the reference image by the complex conjugate of the corresponding pixel in the second image. The burst interferograms are combined into a patch interferogram by appropriately combining pixels from the various burst interferograms in the patch (comb\_int). The resulting patch interferogram is multi-looked, by spatially averaging the complex pixels complex in box about a given pixel, (this is the optimal phase estimation algorithm) to reduce the amount of phase

noise (filt\_int). After the multi-looked interferogram has been generated the phase for each complex sample is computed. Note that the phase measurement is made modulo  $2\pi$ . To generate a continuous height map, the two-dimensional phase field must be unwrapped, that is, the correct multiple of  $2\pi$  must be added to the phase of each pixel so that the relative phase between the pixels will be correct (unw\_rt). After the unwrapping process, there is an overall constant multiple of  $2\pi$  phase offset (that may be zero) that needs to be added to each pixel so that the phase will have the correct relationship (abs\_phase). Estimating this overall phase constant is referred to as absolute phase determination. Subsequent to determining the absolute phase for each pixel in the interferogram the three dimensional target location is determined (height\_recon). In order to accurately position the targets, an accurate baseline estimate is required. In addition phase corrections are applied to the interferometric phase to account for tropospheric effects. A relief map is generated by gridding the unevenly sampled 3-dimensional target locations in a natural coordinate system aligned with the flight path (SCH coordinates). The data are periodically written to disk when the height data from the multiple patches fill a circular buffer containing the final gridded data products (mabuf\_manager).

### 3.1 Range Compression

In the range compression module raw signal data is decoded from 4-bit block floating point quantization (BFPQ) format to floating point. BFPQ is data compression algorithm used to reduce the 8-bit data output from the ADC to 4-bits. The algorithm is structured to preserve the original signal dynamic range by assigning an exponent and mantissa for each sample and reducing the data rate by forcing the exponent to be the same for a group of samples. Data is blocked into groups of 128 samples and an exponent for each block is assigned and each sample in the block is assigned a 4-bit mantissa. This decoding is done via a look up table. Range compression is done using the standard Fourier transform convolution algorithm. A calibration tone was injected into the returned echo data to track phase drift between the inboard and outboard channels that is extracted and stored for use in computing the relative phase between the two interferometric channels. A phase ramp is applied to the reference function of the two channels to remove differential channel delay and correct for an overall phase constant.

### 3.2 Motion Compensation

Motion compensation is the process where the radar signal data are resampled from the actual path of the antenna to an idealized path called the reference path. To motion compensate the data the delta range,  $\Delta\rho$ , from the reference path to the antenna location,  $\vec{d}$ , along the line-of-sight vector,  $\hat{\ell}_R$ , is computed a range and phase correction are applied to each sample using the expressions

$$\Delta\rho \approx \langle \vec{d}, \hat{\ell}_R(\rho, h_{ref}) \rangle, \quad \Delta\phi = \frac{4\pi}{\lambda} \Delta\rho \quad (1)$$

where  $\rho$  is the range,  $\lambda$  is the wavelength, and  $h_{ref}$  is the motion compensation reference height. Motion compensation is done to common reference path which insures the data are co-registered in range after image formation, applies the appropriate range spectral shift for a flat surface and flattens the fringes.

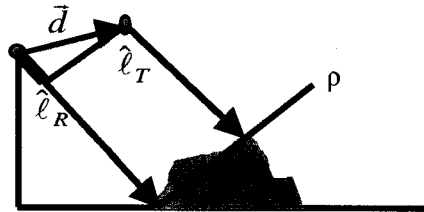


**Figure 4.** A range and phase correction equal to the range difference between the actual and desired path is applied to both channels is shown highlighted in blue.



The need for motion compensation for SRTM can be seen in Figure 5 with shows the motion of the boom and the roll angle of the shuttle after a thruster firings used to maintain the shuttle in mapping attitude. The roll and boom undergo oscillatory motion with an approximate 8 second period with the amplitude decaying as a function of time from the firing. These errors if not properly compensated would generate height errors hundreds of meters in magnitude.

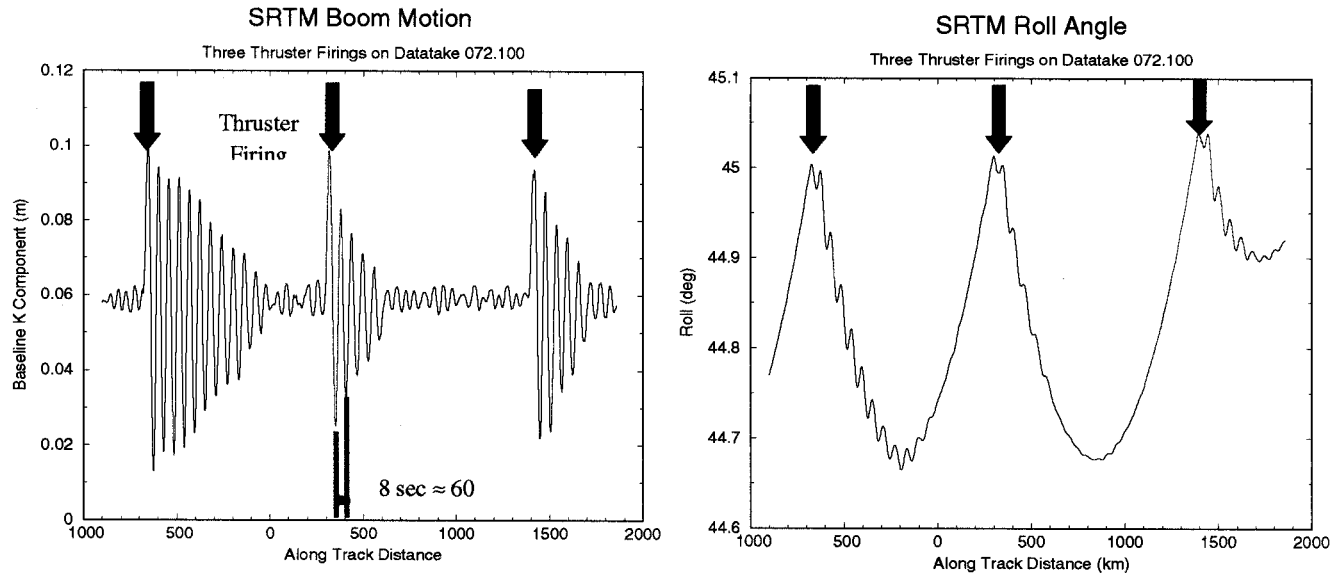


**Figure 5.** Plots showing shuttle roll and boom motion around thruster firings.

### 3.3 Presumming and Azimuth Compression

A number of algorithms can be used for SAR image formation. For SRTM we need an algorithm that can be used with burst mode data and can process the large volume of data efficiently. In addition either through presumming or as part of the azimuth compression process a 7 m along track shift between inboard and outboard antennas must be removed to have the interferometric single look complex data co-registered in azimuth after image formation as illustrated in Figure 6. The processor supports using either a standard range-doppler algorithm or a modified SPECAN<sup>4</sup> algorithm. Because of its computational efficiency modified SPECAN is used for azimuth compression. Included in the algorithm is the ability to compensate for an arbitrary along track offset that is assumed constant for the burst.

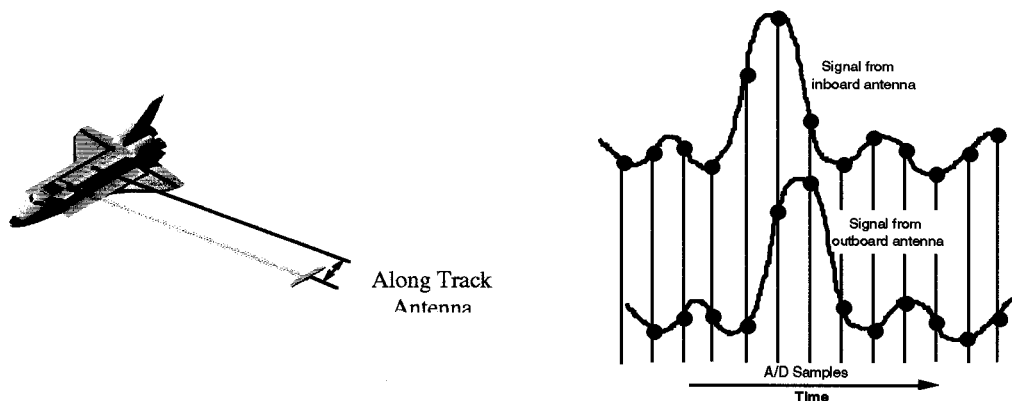


**Figure 6.** The two SRTM interferometric antennas have a 7 m along track shift between as shown in the left portion of the figure. This along track offset between the SRTM antennas causes a time offset between the phase histories as shown right portion of the image. Using either the presummer or by correcting for this offset during azimuth compression insures the image data are co-registered in azimuth.

### 3.4 Interferogram Formation and Filtering

Two methods are possible for generating burst mode interferograms. One method would combine the processed burst complex images into two patch complex images and then form the interferogram. Alternatively, the burst complex images for each channel can be used to generate burst level interferograms and these can be combined to form the patch interferogram. The second method is preferred because the first method has more integrated sidelobe energy (ISLR) and consequently reduces height accuracy. SRTM topographic processor uses the second method for interferogram formation as shown in Figure 8. The number of looks from independent bursts varies spatially and therefore an additional buffer is used to count the number of looks for each pixel in the patch interferogram. The number of looks is typically 1-2 for beam 1 and increases to 2-4 for beam 4. Filtering of the interferogram to reduce noise uses either a boxcar lowpass filter or power spectral filtering<sup>5</sup>.

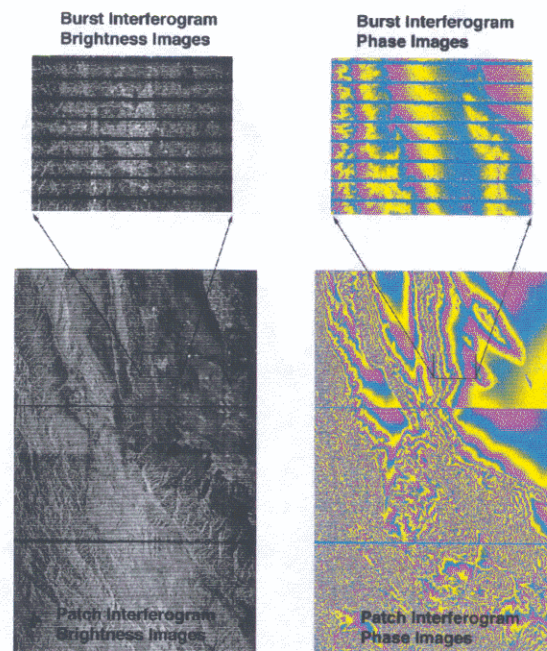


**Figure 8.** Data for each channel is processed and combined to form an interferogram for each burst. The burst interferograms are combined into a patch interferogram. The patch interferogram is filtered to reduce noise prior to the unwrapping process.

### 3.5 Unwrapping and Absolute Phase Determination

Phase unwrapping consists of determining the correct multiple of  $2\pi$  to add to the phase of each point in an interferogram such that the integrated phase along any closed path is constant. Unwrapping uses an updated version of the residue based unwrapping algorithm<sup>6</sup>. The algorithm is patched based so that in principle an infinitely long strip of data could be unwrapped. For each patch the correlation is used to mask out areas of low correlation. Residues are computed to determine points where phase discontinuities exist in the unwrapped phase. Residues are connected if a “tree growing process” to insure that the resulting phase can be recovered without phase discontinuities. The tree growing algorithm uses “neutrons” based on intensity and phase slope to aid in selecting paths to connect the residues. It can happen in the tree growing process that every point in the interferogram can not be connected by a path to any other point without crossing a branch cut. Subregions in the interferogram that can be connected by a continuous path without crossing a branch cut are called connected components. Phase continuity between patches is preserved by retaining a line of phase values in the overlap region that is used to bootstrap the phase from one patch to the next. If the phase variance of the phase values on the overlap line between the two patches on a connected component is smaller than a threshold the bootstrap is considered

successful otherwise the correlation threshold is raised and another unwrapping attempt is made. If correlation threshold is raised to some maximum value without reducing the phase variance sufficiently the region is discarded.

Absolute phase is determined by averaging the unwrapped phase to 500 m postings and then adding multiples of  $2\pi$  and computing the corresponding height values that are compared with the associated height values in a reference low resolution DEM. The multiple of  $2\pi$  with the smallest standard deviation is selected. Usually this algorithm will be run over the ocean at the beginning of each data take where the low resolution DEM value is set to the local geoid height. However, if an isolated connected component of sufficient size is encountered then the absolute phase routine will determine the appropriate multiple of  $2\pi$  using elevation values from the low resolution DEM that was derived from a combination of DTED and ETOPO5 data.

### 3.6 Height Reconstruction and Regridding

Interferometric height reconstruction is the determination of a target's position vector from known platform ephemeris information, baseline information and interferometric phase. Prior to height reconstruction the interferometric phase altered during the motion compensation process is "restored" to the true phase as sensed by the antenna at the time the point was imaged, a process called inverse motion compensation. Correction for dry tropospheric effects on all of the interferometric measurements (range, Doppler and interferometric phase) is made prior to height reconstruction. Certain effects such as multi-path or switch leakage can result in systematic phase distortions that can affect the reconstructed height in 1-10 m range. Provided the multi-path or switch leakage signal resulting in the phase distortions is stable then it can be removed through the use of a phase screen. The phase screen applies a range dependent correction to the interferometric phase. After the phase and range have been corrected for atmosphere and systematic phase distortions the reconstructed target position vector,  $\bar{T}$ , is obtained by solving for the intersection locus of the range sphere centered at the platform position vector,  $\bar{P}$ , the doppler cone with generating axis given by the velocity vector,  $\bar{v}$ , and cone angle a function of the target doppler centroid,  $f$ , and the phase hyperboloid where  $\phi$  is the interferometric phase,  $\rho$  is the range,  $\bar{b}$  is the baseline vector and  $\lambda$  is the wavelength. The simultaneous set of equations is given by

$$\begin{aligned} |\bar{P} - \bar{T}| &= \rho \\ f &= \frac{2}{\lambda} \langle \bar{v}, \hat{\ell} \rangle \\ \phi &= \frac{2\pi}{\lambda} \rho \left( \left( 1 - \frac{2\langle \hat{\ell}, \bar{b} \rangle}{\rho} + \left( \frac{b}{\rho} \right)^2 \right)^{\frac{1}{2}} - 1 \right) \end{aligned} \quad (2)$$

By a clever choice of coordinate systems this non-linear set of equations can be readily solved in closed form.

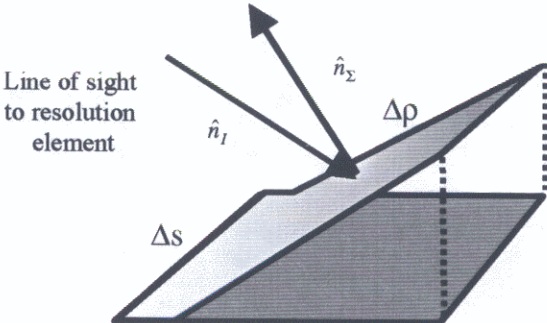
After height reconstruction each unwrapped phase point consists of a triple of numbers, the SCH coordinates of that point. This point does not necessarily lie on an output grid point. Regridding is a resampling of the SCH triples to a uniform grid. Four regridding algorithms included in the processor are nearest neighbor, simplicial, convolutional and surface fitting. Convolutional and surface fitting regridding algorithms also incorporate an adaptive regridding process that adjusts the amount of smoothing depending on the amount of topographic relief compared to the intrinsic measurement noise.

### 3.7 Radiometric Compensation

Although not a requirement for generating topographic maps the amplitude data will be radiometrically corrected to aid in various scientific and classification studies. Radiometric correction is done in four steps. Compensation for the range



squared amplitude reduction is applied immediately after range compression. Burst amplitude data are combined into a patch magnitude image after burst image formation. To avoid an azimuth scalloping of the final amplitude image the azimuth antenna pattern correction is applied for each burst after azimuth compression before it is combined into the patch magnitude image. The elevation antenna pattern correction is applied after height reconstruction when the precise look vector, including terrain effects, is known. Using the look vector and the antenna geometry the precise antenna elevation angle can be computed. An option for correcting the radar backscatter for the ground area is included in the processor. For many applications the corrected backscatter is a more useful quantity. Correction for the area projection factor,  $A$ , is applied during regridding using Equation 3 where  $A$  is the area on the ground responsible for the scattering,  $\Delta\rho$  and  $\Delta s$  are the range and along track resolution element dimensions respectively, and  $\gamma_c$  and  $\gamma_s$  are the cross track and along surface tilts.

$$A = \frac{\Delta\rho\Delta s}{\langle \hat{n}_s, \hat{n}_l \rangle} = \frac{\Delta\rho\Delta s \sqrt{1 - \sin^2(\gamma_c) \sin^2(\gamma_s)}}{\sin(\theta - \gamma_c) \cos(\gamma_s)} \quad (3)$$


**Figure 9.** To obtain a terrain corrected backscatter image the returned signal from a resolution element must be normalized by the ground projected area of the resolution element. The area of the resolution element in the slant plane divided by the dot product of the terrain surface normal and the imaging normal gives the ground projected area. The dot product can be expressed in terms of the local terrain slopes and the look angle as indicated by Equation 3.

#### 4. PROCESSING RESULTS

A nice example of SRTM topographic map data processed during the mission is of the island of Oahu in Hawaii. The Oahu data are from beam 2 and are posted at a 30 m pixel spacing, which is the resolution of the DTED 2 products to be generated by SRTM. These data can be combined with other sensor data shown in Figure 10.

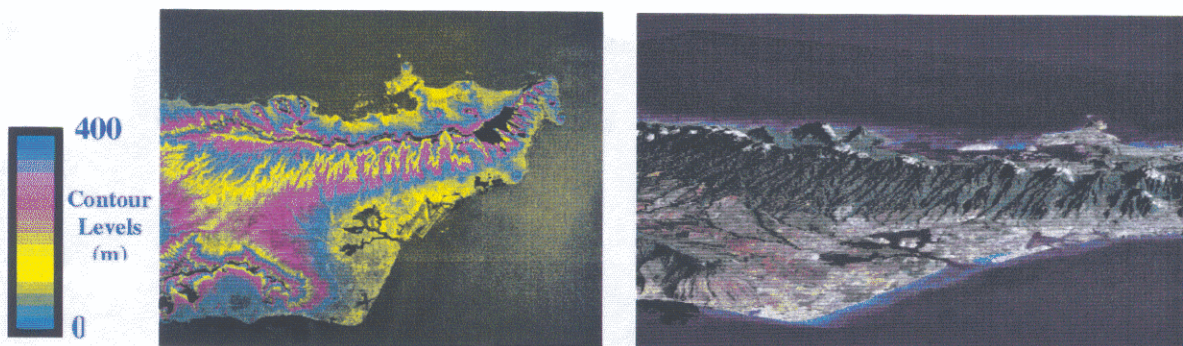


**Figure 10.** The left image of Oahu is combination radar backscatter with color contours overlain. Each color cycle, i.e. going from green to blue and back to green again represents 400 m of elevation change. Honolulu International Airport, Waikiki, and Diamond Head are clearly visible in the image. The right image is a perspective view, using the SRTM generated topography with Landsat imagery overlain.

Using a data collected from a datatake on day four of the mission we processed a strip of data that extended from 100 km north of San Francisco to just south of the tip of Baja, California. The data is posted at 30 m the maximal resolution of the SRTM system. This datatake contains one of our corner reflector calibration arrays deployed in the Mojave Desert just east of Los Angeles. Figure 11 shows 1200 km of processed data from beam 1 with the Los Angeles and San Francisco metropolitan areas highlighted. Note that even in the fairly steep topography of the coastal mountain ranges we obtain good height values. Also observe that we are getting height values over most of the ocean. Processed data from the other beams shows we get sufficient correlation over the ocean to generate height maps except when the ocean is very calm. Urban areas in most of Los Angeles and San Francisco (as well as New York City not shown here), where tall buildings ordinarily would be a problem for interferometric systems, are well mapped by SRTM.

## **5. CONCLUSIONS**

The SRTM Topographic Processor is designed to automatically generate topographic maps using the scans C-band data collected during the SRTM mission. By incorporating several new processing algorithms and giving the user access to a wide variety of processing options makes the processor suitable for robustly processing the variety of terrain types found in a global data set. Results of processing data to date indicate the processor is working as intended and will generate the first globally consistent digital elevation map of the world.

## **ACKNOWLEDGMENTS**

This paper was written at the Jet Propulsion Laboratory, California Institute of Technology, under contract with the National Aeronautics and Space Administration. The authors would like to thank Eric Fielding and Jan Martin for helping process a portion of the data shown in this paper and to thank the AODA team for the prompt and accurate motion data required for processing. We would especially like to thank Scott Shaffer for a many helpful conversations and the Ground Data Processing System Team for generating and formatting the signal data used in this paper.

## **REFERENCES**

1. T. Farr and M. Kobrick, "The Shuttle Radar Topography Mission: A Global DEM, ", IGARSS Proceedings 2000.
2. P. Rosen, S. Hensley, I. Joughin, F. Li, S. Madsen, E. Rodriguez and R. Goldstein, "Synthetic Aperture Radar Interferometry," Proceedings of the IEEE, vol. 88, no 3, March 2000.
3. S. Madsen, H. Zebker, and J. Martin, "Topographic Mapping using radar interferometry: Processing Techniques," IEEE Trans. Geosci. Remote Sensing, vol. 31, pp. 246-256, 1993.
4. R. Lanari, S. Hensley and P. Rosen, "Chirp-Z Transform based SPECAN approach for phase preserving ScanSAR, image generation," Proc. Inst. Elect. Eng. Radar, Sonar, Navig., vol. 145, no. 5, 1998.
5. R. Goldstein and C. Werner, "Radar interferogram filtering for geophysical applications," Geophysical Res. Lett., vol. 25, no. 21, pp. 4035-4038, 1998.
6. R. Goldstein, H. Zebker and C. Werner, "Satellite Radar Interferometry: Two-dimensional phase unwrapping," Radio Sci., vol. 23, no. 4, pp. 713-720, 1988.



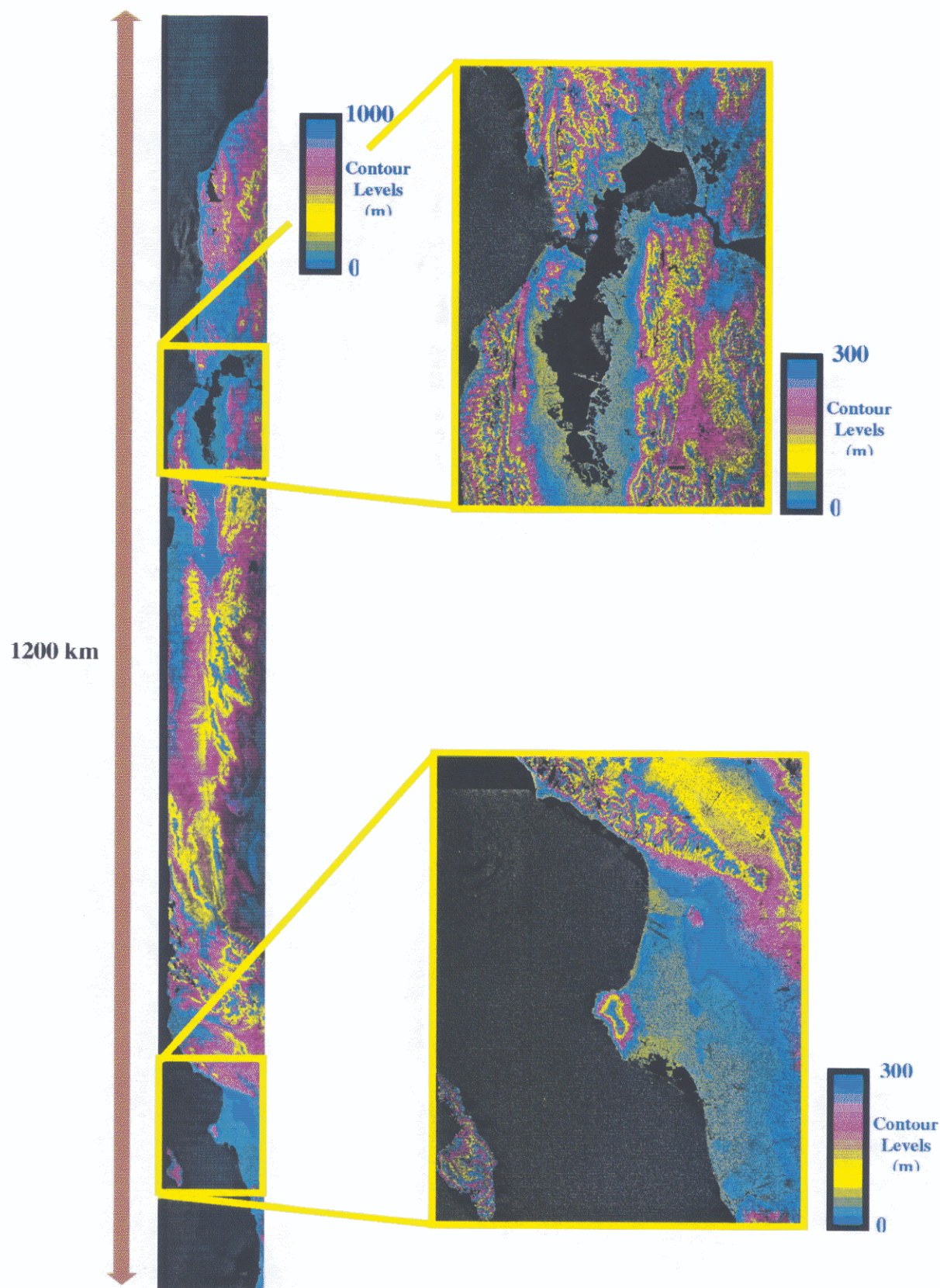


**Figure 11.** Example of a strip map generated using beam 1 data from a descending pass over California. Data are typically processed in regions that do not exceed 1500 km in length. Insets of Los Angeles and San Francisco, the two largest cities in California, show the incredible detail that will be globally available with the SRIM processed data